Am J Transl Res 2023;15(1):138-150
www.ajtr.org /ISSN:1943-8141/AJTR0145199

Original Article

Analysis of serum exosome microRNAs in the rat model of chronic obstructive pulmonary disease

Chao Ouyang*, Wenjun Wang*, Dengfeng Wu, Wei Wang, Xiaoqun Ye, Qing Yang

*Department of Respiratory Diseases, The Second Affiliated Hospital of Nanchang University, Nanchang 330006, Jiangxi, People's Republic of China. *Equal contributors and co-first authors.*

Received July 7, 2022; Accepted December 8, 2022; Epub January 15, 2023; Published January 30, 2023

Abstract: Background: MicroRNAs (miRNAs) play an important role in the pathogenesis of chronic obstructive pulmonary disease (COPD). However, the molecular mechanisms underlying the function of miRNAs remain to be fully understood. This study aimed to explore the profile of serum exosome-derived miRNAs in the rat model of COPD. Methods: We established the COPD rat model by cigarette smoke exposure (CSE). The pulmonary function and morphological changes were analyzed. Serum exosomes were examined by transmission electron microscopy (TEM) and western blotting. The differentially expressed miRNAs between COPD and healthy rats were screened from exosome-derived small RNA library using bioinformatics analysis and experimentally verified in rat lung tissues by quantitative real-time polymerase chain reaction (qRT-PCR). Results: The pulmonary function indexes in COPD rats were significantly decreased compared to control rats. The typical pathological manifestations of emphysema were observed in COPD rats. Marker proteins (CD9, CD63, and TSG101) and characteristic morphology features were detected in serum exosomes. Fifteen differentially expressed miRNAs were identified in the small RNA library. In addition, we confirmed that the expression of miR-185-5p and miR-182-5p was significantly down-regulated in the lung tissues of COPD rats compared to control rats. Conclusion: The expression of miR-185-5p and miR-182-5p was down-regulated in serum-derived exosomes and lung tissues of COPD rats, indicating that these two miRNAs might be involved in the development of COPD and might serve as potential biomarkers for the diagnosis of COPD.

Keywords: Chronic obstructive pulmonary disease (COPD), exosomes, microRNA, bioinformatic analysis

Introduction

Chronic obstructive pulmonary disease (COPD) is a common respiratory disease, ranking as the third leading cause of death worldwide [1]. A total of 384 million people have been diagnosed as COPD worldwide with about 3 million deaths each year, imposing a serious economic and medical burden [2]. Studies have shown that COPD is a chronic inflammatory airway disease which is related to long-term exposure to cigarette smoke or other harmful gases and is characterized by irreversible pulmonary function damage and persistent respiratory symptoms [3]. However, the pathogenesis of COPD and the mechanism of COPD progression have not been fully elucidated, which are critical for the early diagnosis, the development of effective therapies, and the improvement of prognosis.

Exosomes were first discovered in reticulocytes in 1983 and named "exosomes" in 1987 [4]. Exosomes are cystic vesicles secreted by different cells, such as cancer cells, endothelial cells, and macrophagocytes, and are involved in cell-cell communication in various physiological and pathophysiological processes [5]. A variety of substances have been found in exosomes, including proteins, microRNAs (miRNAs), long non-coding RNAs (lncRNAs), and lipids [6]. miRNAs are a class of short-sequence non-coding RNAs of about 21-25 nucleotides long found in eukaryotes and regulate many cellular processes, including cell proliferation, cell migration, epithelial-mesenchymal transformation (EMT), and immune responses [7]. In addition, exosome-derived miRNAs have been found to be involved in the pathogenesis of a lot of diseases and to serve as promising biomarkers for the early diagnosis and the prognosis of these dis-

eases [8, 9]. For example, a study that compared the plasma-derived exosomal miRNAs of 10 lung adenocarcinoma patients and their matched healthy controls has revealed that exosomal miR-23b-3p, miR-10b-5p, and miR-21-5p were significantly and independently related to the poor overall survival of non-small-cell lung cancer (NSCLC) patients [8].

Furthermore, exosomes and miRNAs have been implicated as promising biomarkers for the early detection, severity assessment, and the prognosis prediction of COPD [10-12]. For example, a study has reported the changes in the components of exosomes derived from bronchial epithelial cells exposed to cigarette smoke [10]. Additionally, these exosomes were involved in the enhanced differentiation of myofibroblasts through up-regulating tumor suppressors and hypoxia-inducible factor-1α signaling pathway, which regulates the airway remodeling of COPD [10]. Another study on the role of miRNA in COPD found that miR-181c was down-regulated in the lung tissues of COPD patients compared with individuals who had never smoked [11]. These results demonstrated the importance of exosomes and miRNAs in COPD. Moreover, studies focusing on the exosomal miRNAs in COPD have been carried out [10, 12]. For example, differential expression analysis conducted by DESeq2 has identified distinct plasma-derived extracellular vesicular miRNAs as the expression of miR-22-3p, miR-99a-5p, miR-151a-5p, miR-320b, and miR-320d was up-regulated, while the expression of miR-335-5p, miR-628-3p, miR-887-5p, and miR-937-3p was down-regulated in COPD patients of smokers *vs.* non-smokers [12]. However, differentially expressed miRNAs from serum-derived exosomes in the rat model of COPD and further verification with lung tissues have not yet been carried out.

In this study, we used long-term cigarette smoke exposure (CSE) to construct a rat COPD model to identify the significant serum miRNAs involved in the development of COPD. Pulmonary function tests and histopathological analysis were utilized to evaluate the rat COPD model. In addition, exosomes were isolated from the serum, and differentially expressed exosomes miRNAs were identified by bioinformatics analysis. Furthermore, we experimentally verified the differential expression level of these exosomal miRNAs in the lung tissues of COPD rats. Taken together, our results highlight the importance of exosomes miRNAs in the development of COPD and suggest exosomes miRNAs as potential diagnostic markers of COPD.

Material and methods

Antibodies

Antibodies against CD9, CD63, and TSG101 were purchased from Wuhan Proteintech Biotechnology Co., Ltd. and used at 1:500 dilution.

Animals

Male Sprague-Dawley (SD) rats (age of 8 weeks and weighing about 180±20 g) were obtained from Changsha Tianqin Laboratory Animal Technology Company (Production License: Hunan SCXK2019-0013). These rats were housed in the facility of the Department of Animal Science of Nanchang University under a temperature-controlled environment (22-25°C) with 12-hour light/dark cycle. All rats were fed with standard chow and water. All experiments were performed following the National Institutes of Health (NIH) Guide for the Care and Use of Laboratory Animals and were approved by the Animal Ethical Committee of the Second Affiliated Hospital of Nanchang University.

Establishment of the rat model of COPD and sample collection

As described in **Figure 1**, 20 rats were randomly assigned to two groups, the COPD group (n = 10) and the control group (n = 10). Since long-term cigarette smoke exposure (CSE) was an effective modeling method for COPD as reported previously [13]. The rat in the COPD group were exposed to cigarette smoke, while the control rats were exposed to fresh air. The consecutive CSE was started in September 2020 and ended in December 2020. To enhance the tolerance of animals to CSE, the first week was an acclimation week in which rats were exposed to CSE for only one hour every day. After that, rats in COPD group were exposed to CSE twice a day for 14 weeks. The total CSE time was 15 weeks. Rats were placed in a passive smoking

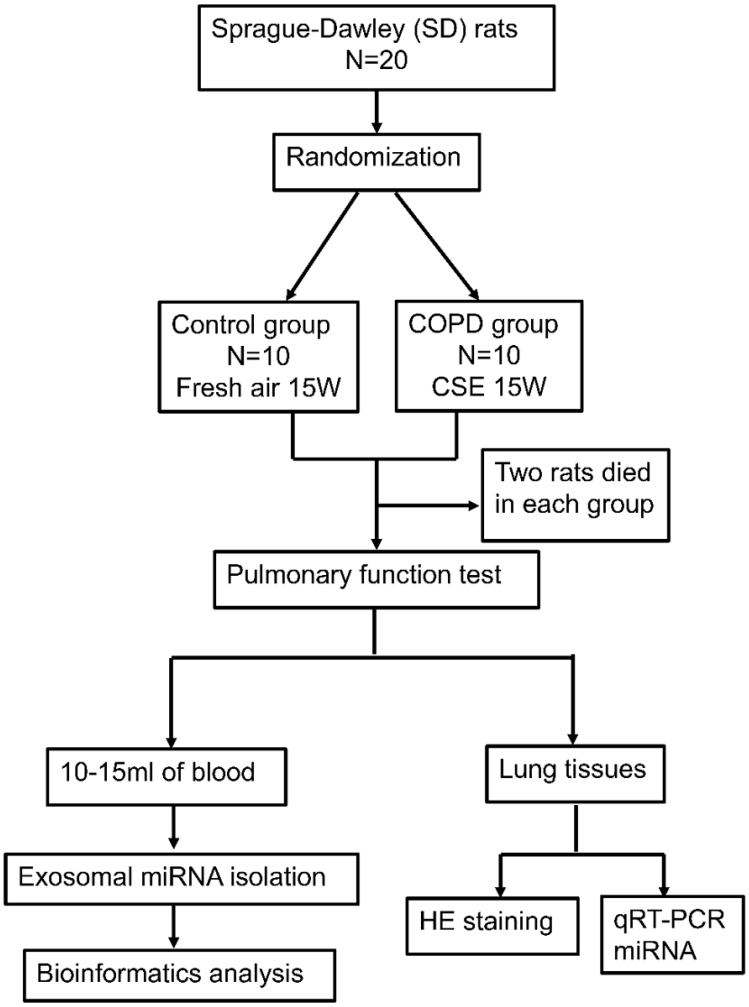

Figure 1. The flowchart of the experiment. COPD: Chronic Obstructive Pulmonary Disease; W: Weeks; CSE: Cigarette Smoke Exposure; HE: Hematoxylin-Eosin; qRT-PCR: Quantitative Real-Time Polymerase Chain Reaction.

animal poisoning system (PAB-S200, Beijing Bestlab High-Tech Co., Ltd., Beijing, China). The smoke was generated by ten commercially available filtered cigarettes (Liqun cigarette containing 1.0 mg of nicotine, 11 mg of carbon monoxide, and 11 mg of tar per cigarette) which were placed towards the cages to create a passive CSE. During the study, two rats in the control group died from bite injuries, while two rats in the COPD group died of respiratory tract inflammation. At the end of the study, pulmonary function test was performed in all rats, and 10-15 mL of blood was extracted from the rat heart under deep anesthesia before the rats were euthanized by decapitation after deep anesthesia. After cardiac arrest and the disappearance of nerve reflex, lung tissues were removed from rats. A portion of lung tissues was frozen at -80°C, and the rest was fixed in 4% paraformaldehyde for further analysis.

Pulmonary function test

A multichannel physiological signal acquisition and processing system (RM-6280XC, Chengdu Instrument Factory, Chengdu, China) was utilized to evaluate the pulmonary function indexes of rats. The animals were anesthetized with pentobarbital sodium intraperitoneal injection (40 mg/kg, Sigma) and were fixed on the operating table. Then, the skin was separated, and the trachea was opened to be connected to the sensor of the instrument. Forced vital capacity (FVC), forced expiratory volume in 300 milliseconds (FEV300) and maximal mid-expiratory flow (MMEF) were detected to evaluate the rats' pulmonary function.

Histological staining and lung tissue morphological analysis

Standard hematoxylin-eosin (HE) staining was used to observe the morphological changes in lung tissues. Briefly, paraffin-embedded lung tissues were sectioned, dewaxed, hydrated, stained with HE, and observed under optical microscope (DP80, Olympus, Tokyo, Japan). The images were analyzed under 200-fold magnification, and three visual fields were randomly selected for analysis per sample. Five alveoli cross-sectional areas (CSA) in one field were measured to calculate the average CSA of this field. The average of the three fields was considered as the CSA of the specimen.

Exosome isolation and identification

Briefly, peripheral blood was collected and placed at room temperature for 30 min before stored at 4°C for 4 h. The clear supernatant

was then obtained by centrifugation at 3000 *g* and 4°C for 15 min twice before subjected to hypervelocity centrifugation (CP100MX, Hitachi, Tokyo, Japan) for exosome purification [14]. The morphology of exosomes was analyzed under transmission electron microscope (TEM) (HT-7700, Hitachi, Tokyo, Japan) as described previously [15]. To confirm the presence of exosomes in the samples, the total protein from exosomes was extracted with RIPA buffer (Wuhan Boster Biological Technology Co., Ltd., Wuhan, China), separated on SDS PAGE, and subjected to western blot analysis with exosomal marker proteins (CD9, CD63, and TSG101). The protein bands were imaged by the Bio-Rad Chemidoc system (Bio-Rad Laboratories, California, USA) and analyzed by Image Lab software (version 6.1).

Exosomal RNA isolation

Total exosomal RNAs were extracted by Trizol reagent following the protocol (Invitrogen, California, USA). MicroRNAs were purified by using miRNeasy Mini kit (Qiagen, Hilden, Germany). cDNAs were synthesized with the PrimeScript RT reagent kit (TaKaRa, California, USA).

Bioinformatics analysis of exosomal miRNAs

QsRNA-seq was carried out for the preparation of sequenced RNA (sRNA) libraries using exosomal miRNA samples. Based on the unique molecular identifiers (UMIs) added to the library construction process, amplification deviation in polymerase chain reaction (PCR) was corrected to accurately quantify exosomal miRNAs. Additionally, Transcripts Per Million (TPM) was utilized to normalize the expression of exosomal miRNAs. The small RNA library was prepared from exosome RNAs isolated from the serum. Raw data (raw reads) of fastq format were first processed through in-house perl scripts. Quality control of the raw reads was performed to acquire high-quality sequences (clean reads) to ensure the accuracy of bioinformatics analysis. Specifically, not only the reads in which the portion of unknown base N (N is an unidentifiable base) was ≥ 10% were excluded, but also the reads without 3' joint sequence were excluded. In addition, the sequences shorter than 15 or longer than 35 nucleotides were excluded. Then, utilizing BowTie Pro (version 1.0), clean reads were executed in the sequence alignment with GtRNAdb database, Silva database, Repbase database, and Rfam database to filter transfer RNA (tRNA), ribosomal RNA (rRNA), small nucleolar RNA (snoRNA), small nuclear RNA (snRNA), and other ncRNAs and repeats. Furthermore, the known miRNAs and novel miRNAs were predicted through comparing to genome and known miRNAs from miRBase. Moreover, Randfold (version 2.0) was utilized for novel miRNA secondary structure prediction. We also performed differential expression analysis using the edgeR package (version 3.12.1). EdgeR provided statistical routines to identify the differential expression in digital miRNA expression data based on the Poisson distribution model and empirical Bayes method. $|\log_2(FC)| \geq 0.584962500721156$ and false discovery rate (FDR) value of < 0.05 were used as the cutoff value. Gene Ontology (GO) enrichment analysis of the genes predicted by differentially expressed miRNAs was implemented by the GO R packages. KOBAS software (version 3.0) was used to test the statistical enrichment of the genes predicted by differentially expressed miRNAs in Kyoto Encyclopedia of Genes and Genomes (KEGG) pathways.

Quantitative real-time PCR (qRT-PCR)

Rat lung tissues were used to verify the differentially expressed miRNAs identified by bioinformatics analysis. The miRNA level was determined by qRT-PCR. Primers used for miRNAs were synthesized by Qiagen (Qiagen, Hilden, Germany). The relative gene expression of miRNAs was calculated by $2^{-\Delta\Delta}$CT. Based on $\log_2(FC)$, the top five differentially expressed miRNAs were selected for verification. The primer sequences of miRNAs used in this study were presented in **Table 1**.

Statistical analysis

Statistical analysis was performed by SPSS software (version 21.0), and figures were created by GraphPad Prism software (version 8.0). All data sets were analyzed for normality by Shapiro-Wilk test. Results were presented as the mean ± standard deviation (SD) for data exhibiting normal distribution. Student's t-test

Table 1. Primer sequences of miRNAs

ID	Orientation	Primer sequences
rno-miRNA-185-5p	Forward	5'-TGGAGAGAAAGGCAGT-3'
rno-miRNA-182-5p	Forward	5'-GCCGAGTTTGGCAATGGTAGAACT-3'
rno-miRNA-1843a-5p	Forward	5'-TATGGAGGTCTCTG-3'
rno-miRNA-1843b-5p	Forward	5'-ATGGAGGTCTCTGTCTG-3'
rno-miRNA-214-3p	Forward	5'-ACAGCAGGCACAGACA-3'
miRNAs	Reverse	5'-CAGTGCAGGGTCCGAGGTAT-3'
U6	Forward	5'-CTCGCTTCGGCAGCACA-3'
U6	Reverse	5'-AACGCTTCACGAATTTGCGT-3'
GAPDH	Forward	5'-CAAGGTCATCCATGACAACTTTG-3'
GAPDH	Reverse	5'-GTCCACCACCCTGTTGCTGTAG-3'

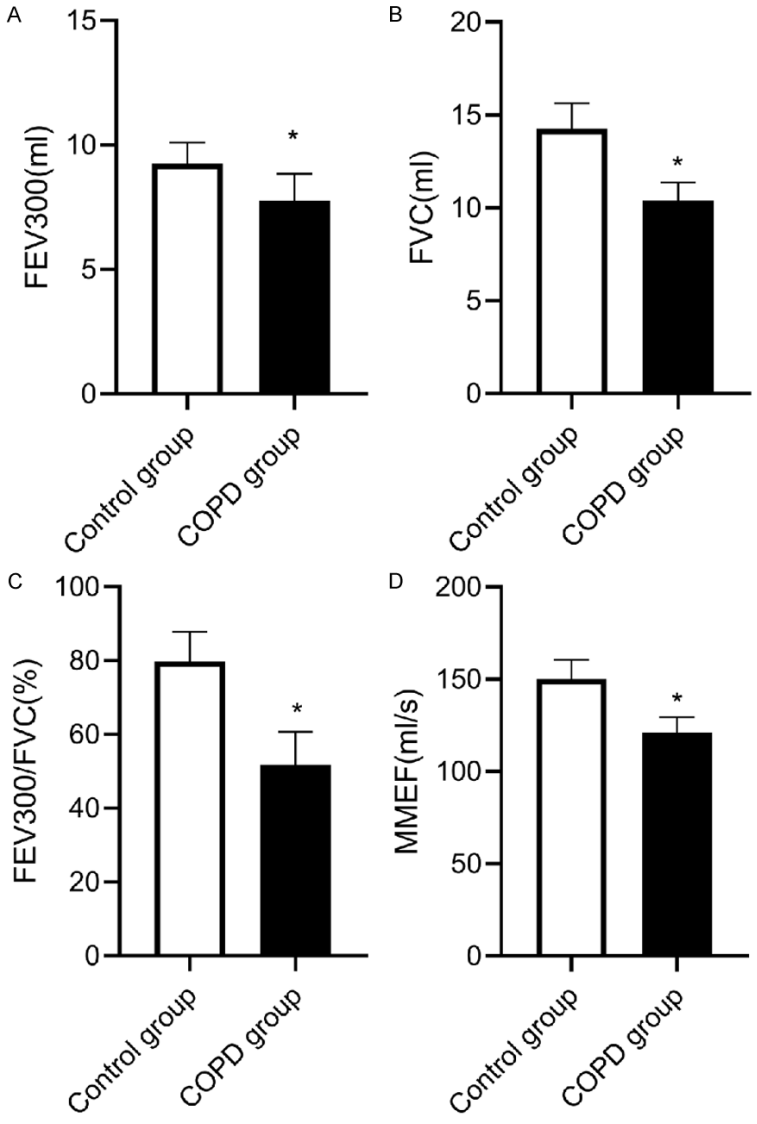

Figure 2. Pulmonary function indexes of rats in the two groups. A: FEV300 of the two groups. B: FVC of the two groups. C: FEV300/FVC of the two groups. D: MMEF of the two groups. COPD: Chronic Obstructive Pulmonary Disease; FVC: Forced Vital Capacity; FEV300: Forced Expiratory Volume in 300 milliseconds; MMEF: Maximal Mid-Expiratory Flow. *P < 0.05.

was used to compare the difference between two groups. Rank-sum test was utilized for non-normally distributed data. A *P* value of < 0.05 was considered statistically significant.

Results

Phenotypical analysis of COPD rats

As CSE intervention progressed, the COPD rats exhibited sluggish activity, sweat, and shortness of breath, which were more obvious with mouth breathing and coughing. In addition, the hair of the COPD rats was partly lost, and the color of furs also turned yellow. Furthermore, the food and water intake of the COPD rats decreased. In contrast, the control rats presented no irritation, and their respiratory rhythm, diet, and hair color remained unchanged.

A pulmonary function test was conducted on every rat to assess the effect of long-term CSE. Compared to the control rats, the pulmonary function indexes (FEV300, FVC, FVE300/FVC, and MMEF) were all lower in the COPD rats (P < 0.05, **Figure 2**), indicating that CSE obviously damaged the pulmonary function of COPD rats.

We further examined the morphology of lung tissues and observed the typical pathological changes in COPD rats such as the thickened bronchial wall of the small airways and the inflammatory cells around the airways (**Figure 3B**). Additionally, the disturbed alveolar structure, the thinned or broken alveolar wall, and the enlarged alveolar cavity were also observed in the COPD rats

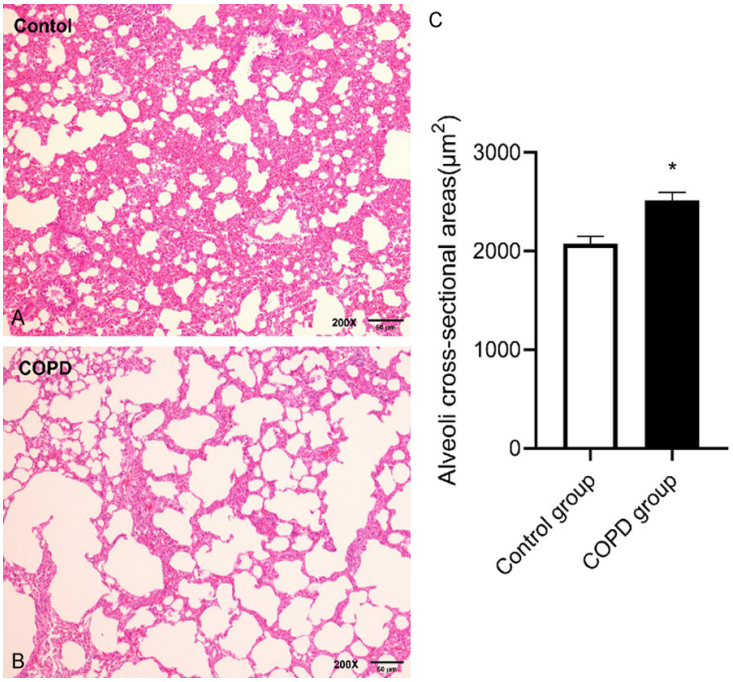

Figure 3. Histological structure of lung tissues. A: Histological structure of lung tissues in control rats. Magnification: × 200. Scale bar = 50 μm. B: Histological structure of lung tissues in COPD rats. Magnification: × 200. Scale bar = 50 μm. C: Comparison of the alveolar cross-sectional area between the two groups. *P < 0.05. COPD: Chronic Obstructive Pulmonary Disease.

(**Figure 3B**). However, in the control rats, there was no obvious fracture or thickening and no inflammatory cell infiltration in the small airway wall, and the alveolar structure was normal (**Figure 3A**). Moreover, the alveolar CSA in the COPD rats was higher than that in the control rats (P < 0.05, **Figure 3C**).

Serum exosomes isolation and analysis

We compared the structure of exosomes between COPD rats and control rats. In both groups, the exosomes were spherical and relatively uniform in size under the TEM (**Figure 4A** and **4B**). NanoSight analysis showed that the diameter distribution of exosomes ranged from 40 to 140 nm, and the percentage of the diameter distribution in the two groups was almost identical (**Figure 4C**). Moreover, western blot analysis identified the expression of exosome marker proteins (CD9, CD63, and TSG101) in these samples (**Figure 4D**).

Bioinformatics analysis of exosomal miRNAs

We performed bioinformatics analysis and identified 15 differentially expressed miRNAs (8 up-regulated miRNAs and 7 down-regulated miRNAs) between rats in these two groups, which were presented on the volcano plot (**Figure 5**). Except for the two up-regulated unknown miRNAs, the other 13 exosomal miRNAs were displayed in **Table 2**. The seven down-regulated miRNAs were rno-miRNA-185-5p, rno-miRNA-182-5p, rno-miRNA-214-3p, rno-miRNA-183-5p, rno-miRNA-20b-5p, rno-miRNA-221-3p, and rno-miRNA-122-5p, while the six up-regulated miRNAs were rno-miRNA-1843a-5p, rno-miRNA-1843b-5p, rno-miRNA-206-3p, rno-miRNA-1-b, rno-miRNA-1-3p, and rno-miRNA-133a-3p. We also predicted the target genes for these 13 differentially expressed miRNAs as shown in **Table 3**.

GO enrichment and KEGG signaling pathway analyses of target genes on these differentially expressed exosomal miRNAs were conducted. GO analysis revealed the enrichments of three biological processes (**Figure 6A**), cell components (**Figure 6B**), and molecular functions (**Figure 6C**). Seven biological processes were significantly enriched, including positive regulation of transcription from RNA polymerase II promoter, negative regulation of transcription from RNA polymerase II promoter, positive regulation of transcription, DNA-templated, positive regulation of GTPase activity, regulation of ion transmembrane transport, negative regulation of transforming growth factor-beta receptor signaling pathway, and skeletal system development (**Figure 6A**). We found that 10 cell components were significantly enriched, including postsynaptic density, neuronal cell body, cell junction, receptor complex, dendrite, cytoplasm, actin cytoskeleton, postsynaptic membrane, Golgi membrane, and lamellipodium (**Figure 6B**). The following 10 molecular functions were significantly enriched: adenosine triphosphate (ATP) binding, zinc ion binding, chromatin binding, RNA polymerase II proximal promoter sequence-specific DNA binding, GTPase activator activity, RNA polymerase II proximal promoter sequence-specific

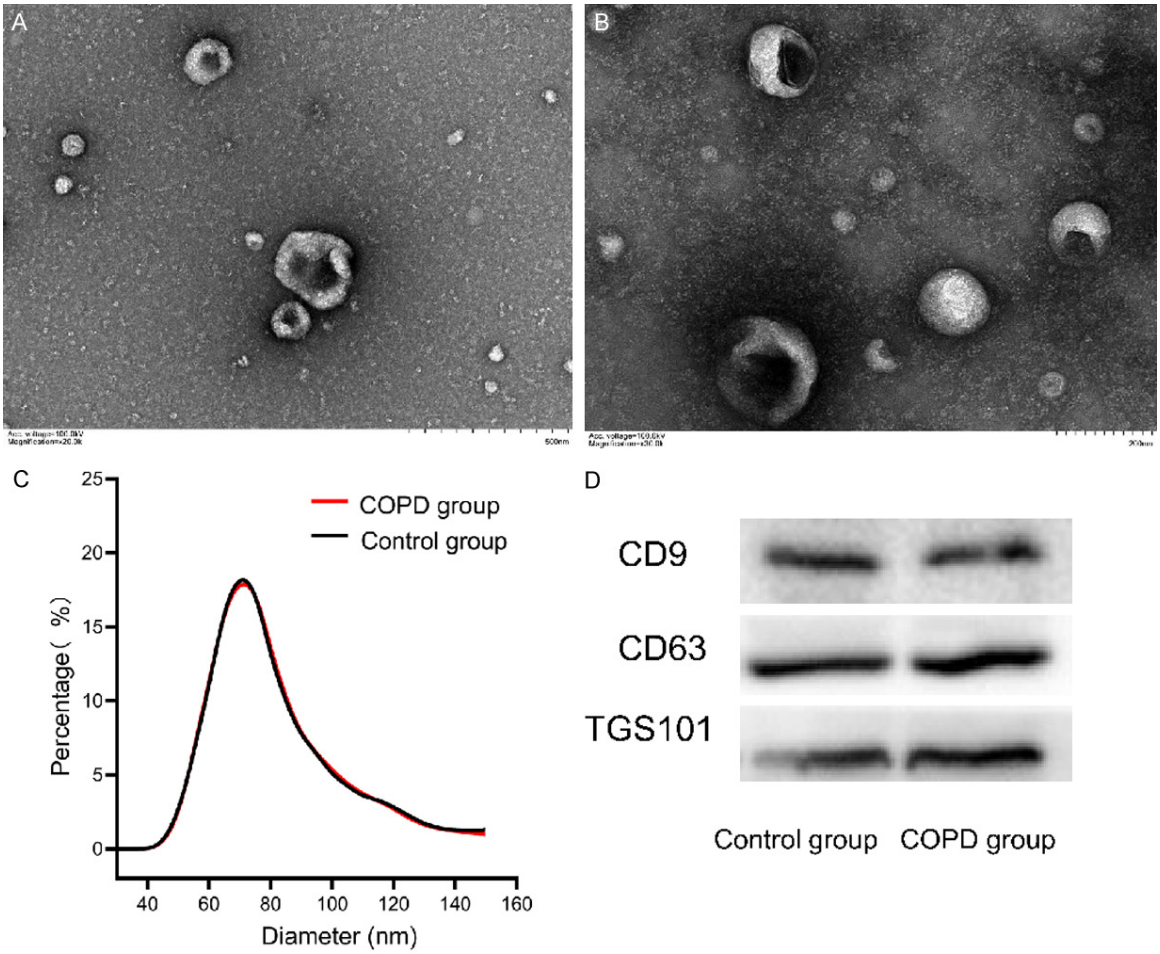

Figure 4. Characterization of serum exosomes derived from rats in the two groups. A: Morphology of exosomes, scale bar = 500 nm. B: Morphology of exosomes, scale bar = 200 nm. C: The diameter distribution of serum exosomes in the two groups. D: The expression of exosomal marker proteins: CD9, CD63, and TSG101. COPD: Chronic Obstructive Pulmonary Disease.

DNA binding, sequence-specific DNA binding, metal ion binding, protein kinase binding, and RNA polymerase II transcription factor activity (**Figure 6C**). The top 20 KEGG signaling pathways associated with these miRNAs were MAPK signaling pathway, axon guidance, glutamatergic synapse, endocytosis, dilated cardiomyopathy, oxytocin signaling pathway, focal adhesion, pathways in cancer, microRNAs in cancer, GABAergic synapse, arrhythmogenic right ventricular cardiomyopathy, PI3K-Akt signaling pathway, FoxO signaling pathway, circadian entrainment, proteoglycans in cancer, retrograde endocannabinoid signaling, extracellular matrix-receptor interaction, transcriptional mis-regulation in cancer, Ras signaling pathway, and GnRH signaling pathway (**Figure 6D**). All p values were < 0.05.

Verification of differentially expressed miRNAs by qRT-PCR

From bioinformatics analysis, 5 miRNAs, including rno-miRNA-185-5p, rno-miRNA-182-5p, rno-miRNA-1843a-5p, rno-miRNA-1843b-5p, and rno-miRNA-214-3p, were identified as the top five differentially expressed miRNAs between COPD and control group rats. We then experimentally validated this result in lung tissues by qRT-PCR. Among them, the expression of rno-miRNA-1843a-5p was extremely low in both groups, which was excluded from further analysis. The expression of rno-miRNA-185-5p and rno-miRNA-182-5p was significantly lower in the lung tissues of COPD rats than that of control rats ($P < 0.05$, **Figure 7A** and **7B**). However, the expression of rno-miRNA-1843b-

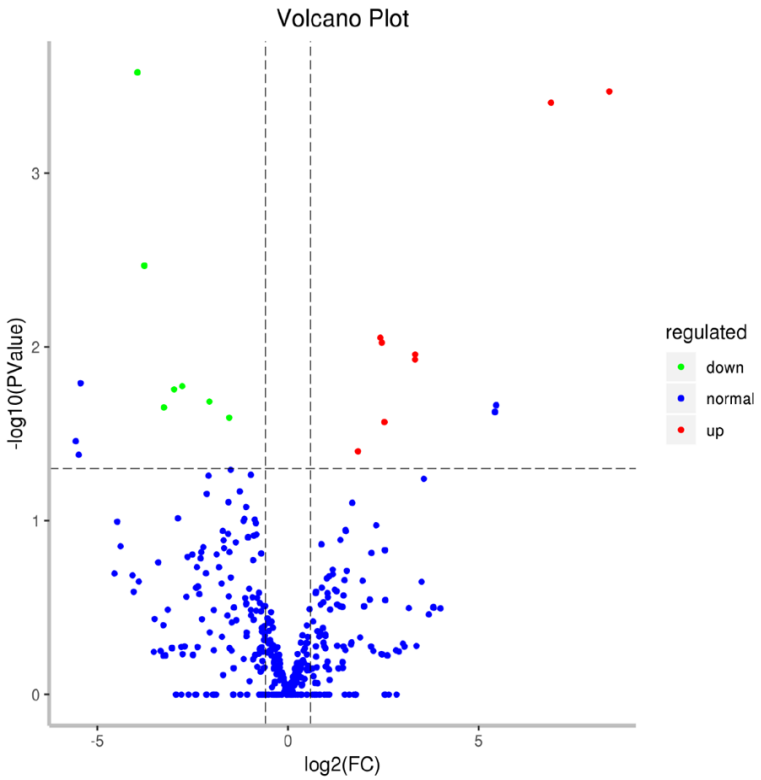

Figure 5. Differentially expressed exosomal miRNAs between the two groups, which was visualized by volcano plot.

Table 2. Differentially expressed exosomal miRNAs between the two groups

ID	False discovery rate (FDR) Value	log_2(FC)	Regulation
rno-miRNA-185-5p	0.0002631255	3.9436890428	down
rno-miRNA-182-5p	0.0034008831	3.7639013408	down
rno-miRNA-1843a-5p	0.0073710707	3.3334493873	up
rno-miRNA-1843b-5p	0.0118173479	3.3303379701	up
rno-miRNA-214-3p	0.0222977659	3.2528878810	down
rno-miRNA-183-5p	0.0175177892	2.9833260937	down
rno-miRNA-20b-5p	0.0168263766	2.7734000581	down
rno-miRNA-206-3p	0.0270485281	2.5252089760	up
rno-miRNA-1-b	0.0094377401	2.4562624443	up
rno-miRNA-1-3p	0.0088476963	2.4206143470	up
rno-miRNA-221-3p	0.0206170504	2.0600218250	down
rno-miRNA-133a-3p	0.0398251446	1.8346564169	up
rno-miRNA-122-5p	0.0255105868	1.5394332695	down

5p and rno-miRNA-214-3p in lung tissues had no difference between the two groups ($P < 0.05$, **Figure 7C** and **7D**).

Discussion

Since cigarette smoke is the main risk factor for the development of COPD, passive CSE has been used as the standard animal model of COPD [16]. Previous studies found that CSE of 8-10 cigarettes/day, 7 days/week, for 12-16 weeks was an effective and tolerable modeling method [13, 17]. Consistently, our study also showed that the pulmonary function indexes decline in COPD rats after CSE, an indicator of the development of COPD.

Exosomes are single-membrane secreted organelles with 30-200 nm in diameter [18]. The exosome protein markers include fusion proteins, membrane transporter proteins, heat shock proteins, and quad transmembrane protein superfamily such as CD9 and CD63 [19]. In this study, the diameter of serum exosomes ranged from 40 to 140 nm, and maker proteins (CD9 and CD63) were positively expressed, indicating that these exosomes were suitable for further analysis.

Our study found 15 differently expressed exosomal miRNAs that might be involved in the development of COPD. Emerging studies have shown that exosomal miRNAs not only serve as biomarkers but also participate in the pathogenesis of COPD [20-22]. For example, one previous study reported that, compared to phosphate-buffered saline (PBS) treatment, CSE treatment enhanced the expression of exosomal miR-210 in human bronchial epithelial cells, which might act as a para-

Table 3. Prediction of target genes for differentially expressed exosomal miRNAs

ID	Target genes
rno-miRNA-185-5p	*Myo18b; Large2; Eda; Phyhip; LOC103690098; LOC102555189; Clec2l; Git1; Zfp362; Prkd3; Htra4; Nif3l1; Gin1; Gsdma; Galnt2; Edem1; Adarb1; Odf2; Zfp94; Hn1l; Ccdc71l; Rgs7bp; Sphkap; Elof1; Zfp609; Tmem63c; LOC100911196; Crygd; Lmbr1; Cacna1d; Nucb1; LOC103690141; LOC108348161; Insrr; Sap25; Tcf12; Ovol1*
rno-miRNA-182-5p	*Slc2a3; LOC100909595; Taok2; Cobl*
rno-miRNA-1843a-5p	*LOC683404; Elfn1; Alpp; Tmtc1; Traf7; Fcgbpl1; Phc3; Tnfaip2*
rno-miRNA-1843b-5p	*Dzip1; Samd10; Alms1; Arhgap23; Crispld1; Ift88; Cer1; Rbm25; Mnda; Gdf10; Setd2; Traf7; Hip1r; Tnfaip2; Pkd1*
rno-miRNA-214-3p	*Lmo3; Ptcd2; Zzz3; Apeh; Fam193a; Aacs; LOC499240; Lrba; Abt1; Kpna3; Sptbn5; Pkhd1l1; Lrp1; Anapc1; Lmo1; Agpat1; Rcc2; rf1; Mia3; Uba7; Ugt1a1; Papd7; Suv39h2; Dlk2; LOC102546589; Tpd52; Nkain4; Supt3h; Stam; Fam134a; Nrg1; LOC691083; Lrp5; Rfng; Map2; LOC689081; Slc45a4; Ciz1; Mybbp1a; Smad3; Cdc42se1*
rno-miRNA-183-5p	*Dcaf5*
rno-miRNA-20b-5p	*Tnfsf12; LOC690299; Adamts15*
rno-miRNA-206-3p	*Miga2; LOC100911428*
rno-miRNA-1-b	-
rno-miRNA-1-3p	-
rno-miRNA-221-3p	*Pml*
rno-miRNA-133a-3p	*Ptpn4; Card10; Zzef1; Lilrb3*
rno-miRNA-122-5p	*Mapkapk3; MGC95210; Myo1h; Tshz3; Zfp169; Kcnd2*

crine autophagy mediator for regulating the differentiation of myofibroblast [22]. Another study showed that miR-122-5p in the lung-derived exosomes of COPD patients was three-fold down-regulated compared with healthy non-smokers control and five-fold down-regulated compared with healthy smokers, indicating the potential role of exosomal miRNAs as biomarkers in COPD [20]. Interesting results were also reported that when comparing miRNAs level in plasma exosomes derived from cigarette smokers, water pipe smokers, dual smokers (cigarette and water pipe) and healthy non-smokers, seven miRNAs (hsa-let-7a-5p, hsa-miR-21-5p, hsa-miR-29b-3p, hsa-let-7f-5p, hsa-miR-143-3p, hsa-miR-30a-5p and hsa-let-7i-5p) were differentially expressed between all smoking groups and non-smokers [21]. However, when compared cigarette smokers group with non-smoker group, five differentially expressed miRNAs (hsa-miR-224-5p, hsa-miR-193b-3p, hsa-miR-30e-5p, hsa-miR-423-3p, hsa-miR-365a-3p, and hsa-miR-365b-3p) were detected, which were not expressed in other three groups [21]. Collectively, these results indicate the important role of exosomal miRNAs in COPD.

In our study, we revealed that the levels of rno-miRNA-185-5p and rno-miRNA-182-5p were significantly lower in COPD rats than those in control rats. The function of miRNA-185-5p has been studied in cancer [23, 24]. For example, a study showed that miR-185-5p suppressed tumor cell-derived exosome-mediated proliferation, invasion, and migration of NSCLC cells by down-regulating RAB35 [23]. Our study was the first to report that miR-185-5p might be involved in the development of COPD. Other important functions of miR-185-5p have been reported too. Serum miR-185-5p level has been suggested as a biomarker for the early diagnosis of asthma [25]. Further mechanistic study showed that the downregulation of miR-185-5p enhanced the expression of periostin in bronchial smooth muscle cells and small airway epithelial cells, which regulated smooth muscle contraction in asthma [26]. Furthermore, compared with healthy controls, a decrease in miR-185-5p expression in sputum cells from asthmatics was detected, consistent with our result that miR-185-5p was declined in COPD [26]. Moreover, bioinformatics analysis of lung tissues between pulmonary arterial hypertension patients and healthy controls

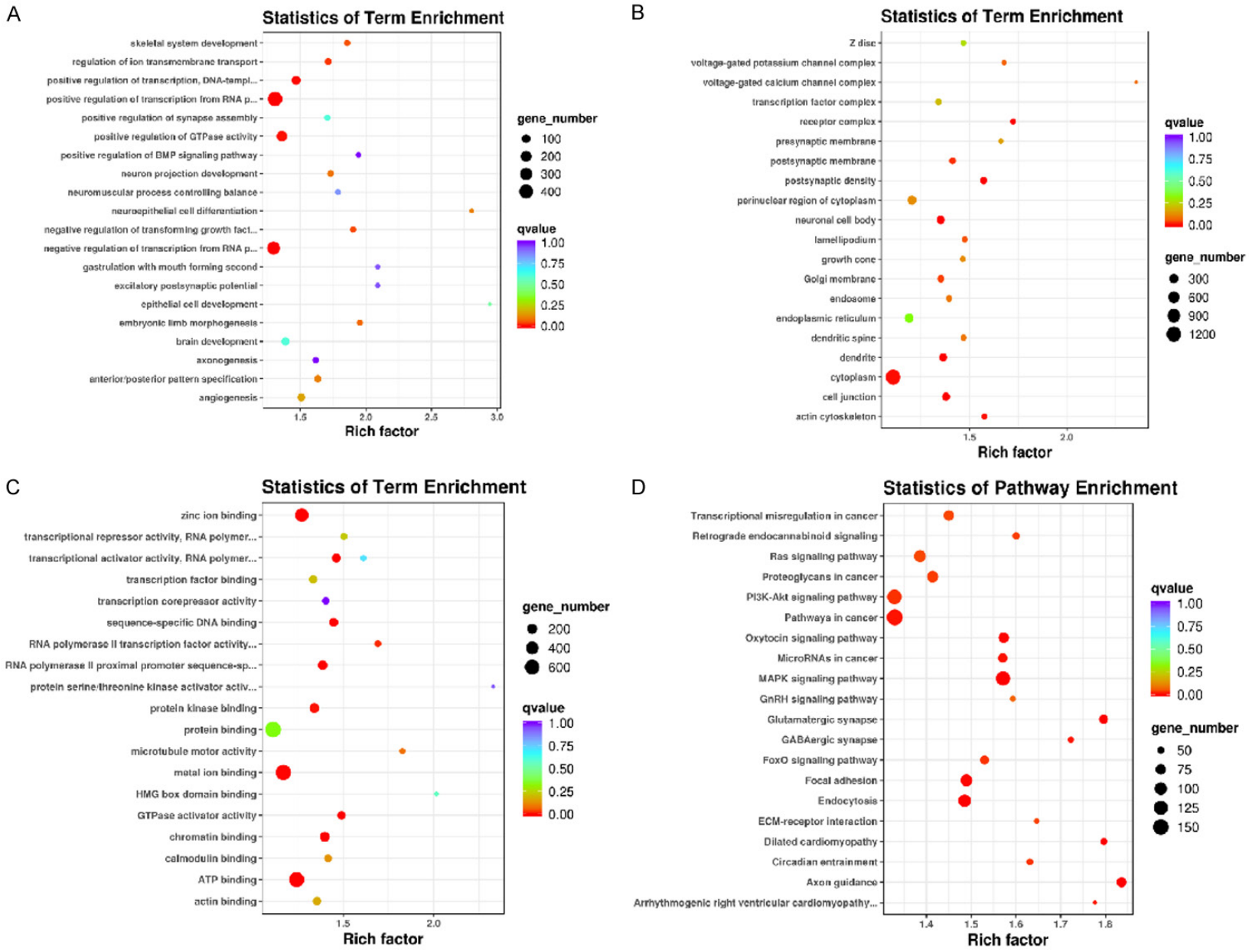
A
Statistics of Term Enrichment
skeletal system development
regulation of ion transmembrane transport
positive regulation of transcription, DNA-templ...
positive regulation of transcription from RNA p...
positive regulation of synapse assembly
positive regulation of GTPase activity
positive regulation of BMP signaling pathway
neuron projection development
neuromuscular process controlling balance
neuroepithelial cell differentiation
negative regulation of transforming growth fact...
negative regulation of transcription from RNA p...
gastrulation with mouth forming second
excitatory postsynaptic potential
epithelial cell development
embryonic limb morphogenesis
brain development
axonogenesis
anterior/posterior pattern specification
angiogenesis
1.5
2.0
2.5
3.0
Rich factor
gene_number
100
200
300
400
qvalue
1.00
0.75
0.50
0.25
0.00
B
Statistics of Term Enrichment
Z disc
voltage-gated potassium channel complex
voltage-gated calcium channel complex
transcription factor complex
receptor complex
presynaptic membrane
postsynaptic membrane
postsynaptic density
perinuclear region of cytoplasm
neuronal cell body
lamellipodium
growth cone
Golgi membrane
endosome
endoplasmic reticulum
dendritic spine
dendrite
cytoplasm
cell junction
actin cytoskeleton
1.5
2.0
Rich factor
qvalue
1.00
0.75
0.50
0.25
0.00
gene_number
300
600
900
1200
C
Statistics of Term Enrichment
zinc ion binding
transcriptional repressor activity, RNA polymer...
transcriptional activator activity, RNA polymer...
transcription factor binding
transcription corepressor activity
sequence-specific DNA binding
RNA polymerase II transcription factor activity...
RNA polymerase II proximal promoter sequence-sp...
protein serine/threonine kinase activator activ...
protein kinase binding
protein binding
microtubule motor activity
metal ion binding
HMG box domain binding
GTPase activator activity
chromatin binding
calmodulin binding
ATP binding
actin binding
1.5
2.0
Rich factor
gene_number
200
400
600
qvalue
1.00
0.75
0.50
0.25
0.00
D
Statistics of Pathway Enrichment
Transcriptional misregulation in cancer
Retrograde endocannabinoid signaling
Ras signaling pathway
Proteoglycans in cancer
PI3K-Akt signaling pathway
Pathwaya in cancer
Oxytocin signaling pathway
MicroRNAs in cancer
MAPK signaling pathway
GnRH signaling pathway
Glutamatergic synapse
GABAergic synapse
FoxO signaling pathway
Focal adhesion
Endocytosis
ECM-receptor interaction
Dilated cardiomyopathy
Circadian entrainment
Axon guidance
Arrhythmogenic right ventricular cardiomyopathy...
1.4
1.5
1.6
1.7
1.8
Rich factor
qvalue
1.00
0.75
0.50
0.25
0.00
gene_number
50
75
100
125
150

Figure 6. GO enrichment and KEGG signaling pathway analyses of the predicted target genes of the differentially expressed exosomal miRNAs. A: GO enrichment analysis of target genes predicted by differentially expressed miRNAs from biological processes. B: GO enrichment analysis of target genes predicted by differentially expressed miRNAs from cell components. C: GO enrichment analysis of target genes predicted by differentially expressed miRNAs from molecular functions. D: KEGG signaling pathway analysis of target genes predicted by differentially expressed exosomal miRNAs. GO: Gene Ontology; KEGG: Kyoto Encyclopedia of Genes and Genomes.

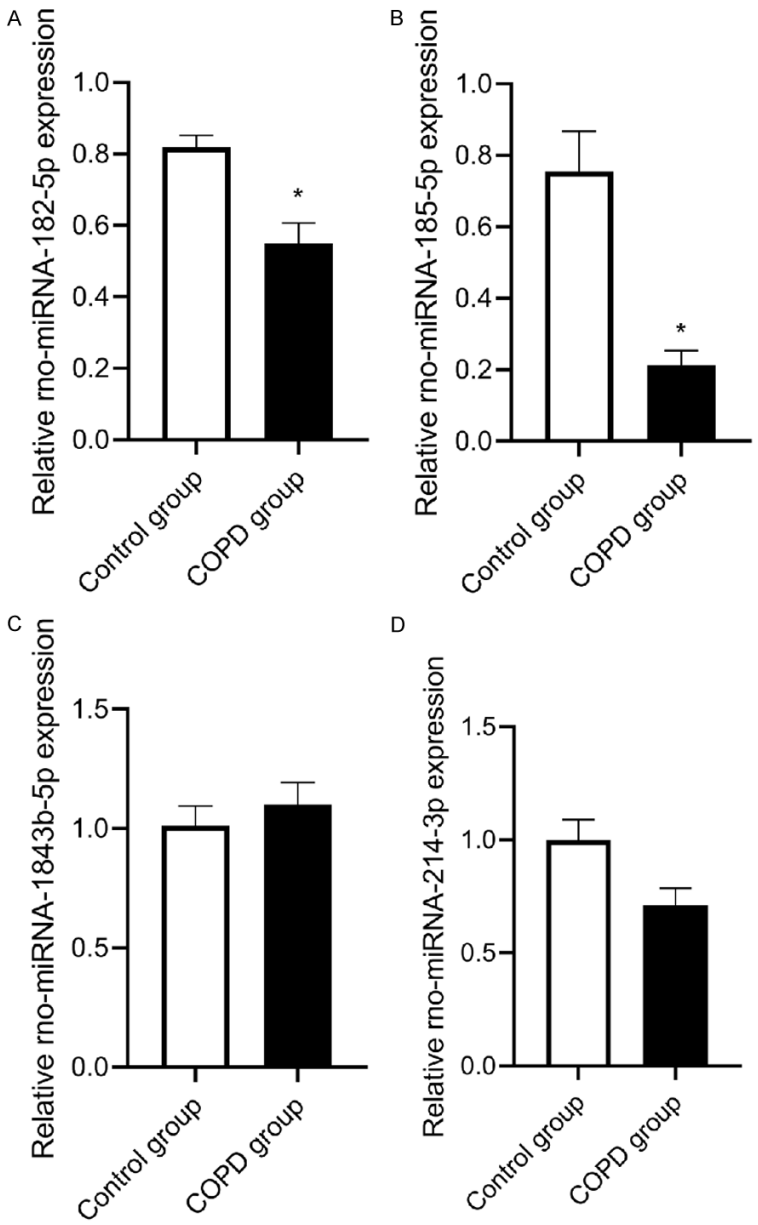

Figure 7. The verification of differentially expressed miRNAs by qRT-PCR in lung tissues of the two groups. (A-D) The relative expression of rno-miRNA-182-5p (A), rno-miRNA-185-5p (B), rno-miRNA-1843b-5p (C), and rno-miRNA-214-3p (D). *P < 0.05. COPD: Chronic Obstructive Pulmonary Disease; qRT-PCR: quantitative Real-Time Polymerase Chain Reaction.

revealed that the predicted target genes of these differentially expressed miRNAs (miR-103a-3p, miR-185-5p, and miR-515-5p) were strongly related to idiopathic pulmonary arterial hypertension [27]. Exosomal miR-185-5p was also studied in bronchopulmonary dysplasia [28]. When analyzing the exosomal miRNAs from bronchoalveolar lavage fluid of bronchopulmonary dysplasia patients, a decreased expression of hsa-miR-103a-3p and hsa-miR-185-5p was found in patient samples compared to healthy controls [28]. These results, together with our results, indicate the involvement of miR-185-5p in the physiological and pathophysiological processes, such as airway development and remodeling.

Similar to miR-185-5p, the function of miRNA-182-5p is mainly studied in cancer [29, 30]. For example, the upregulation of miR-182-5p is reported to be strongly related to the early recurrence and poor prognosis of patients with hepatocellular carcinoma who have undergone curative surgery, and miR-182-5p enhances the motility and the invasive ability of hepatocellular carcinoma cells both *in vitro* and *in vivo* [30]. However, only few studies explore the function of miR-182-5p in COPD. Our study was the first to determine the functional connection between them. Our study was based on several previous findings. First, it was reported that miR-182-5p was related to pulmonary diseases and that miR-182-5p was overexpressed in the lung tis-

sues of bleomycin (BLM)-induced fibrotic mice model. Second, downregulation of miR-182-5p suppressed the level of profibrotic proteins including fibronectin, α-smooth muscle actin, and p-Smad2/p-Smad3, which suppressed pulmonary fibrosis [31]. In addition, miR-182-5p inhibited tumor necrosis factor (TNF)-α-induced proliferation and migration of airway smooth muscle cells by decreasing the activation of nuclear factor-κB (NF-κB) via targeting TRIM8, indicating the potential role of miR-182-5p in the airway remodeling of asthma [32]. Furthermore, mesenchymal stem cells-derived exosomes transmitted miR-23a-3p and miR-182-5p which were involved in reversing the epithelial-mesenchymal transition (EMT) during lipopolysaccharide (LPS)-induced lung injury and fibrosis [33]. These findings suggest that miR-182-5p is involved in EMT and the airway remodeling of lung, which plays a similar role in the development of COPD.

In summary, we employed a small RNA-sequencing analysis to identify the differentially expressed exosomal miRNAs in the rat model of COPD. Our data suggested that miR-185-5p and miR-182-5p might be involved in the pathogenesis of COPD and might serve as potential biomarkers for the diagnosis of COPD. However, there are some limitations in this study. First, the number of animals was small; hence our results need to be validated with larger sample size. Second, we used lung tissue to verify the differential expression of blood-derived exosomal miRNA, which should be further validated using the blood samples of COPD patients. Nevertheless, two miRNAs presented in this article could be new targets for the subsequent study on the mechanism of COPD.

Acknowledgements

This work was supported by the grant from National Natural Science Foundation of China (No: 81860011).

Disclosure of conflict of interest

None.

Address correspondence to: Qing Yang, Department of Respiratory Diseases, The Second Affiliated Hospital of Nanchang University, No. 1 Minde Road, Nanchang 330006, Jiangxi, People's Republic of China. Tel: +86-18170807068; Fax: +86-0791-6300507; E-mail: lisaqing2004@126.com

References

[1] Vogelmeier CF, Román-Rodríguez M, Singh D, Han MK, Rodríguez-Roisin R and Ferguson GT. Goals of COPD treatment: focus on symptoms and exacerbations. Respir Med 2020; 166: 105938.

[2] Rabe KF and Watz H. Chronic obstructive pulmonary disease. Lancet 2017; 389: 1931-1940.

[3] Labaki WW and Rosenberg SR. Chronic obstructive pulmonary disease. Ann Intern Med 2020; 173: ITC17-ITC32.

[4] Johnstone RM, Adam M, Hammond JR, Orr L and Turbide C. Vesicle formation during reticulocyte maturation. Association of plasma membrane activities with released vesicles (exosomes). J Biol Chem 1987; 262: 9412-9420.

[5] Mathivanan S, Ji H and Simpson RJ. Exosomes: extracellular organelles important in intercellular communication. J Proteomics 2010; 73: 1907-1920.

[6] Wang N, Wang Q, Du T, Gabriel ANA, Wang X, Sun L, Li X, Xu K, Jiang X and Zhang Y. The potential roles of exosomes in chronic obstructive pulmonary disease. Front Med (Lausanne) 2021; 7: 618506.

[7] Bartel DP. Metazoan microRNAs. Cell 2018; 173: 20-51.

[8] Liu Q, Yu Z, Yuan S, Xie W, Li C, Hu Z, Xiang Y, Wu N, Wu L, Bai L and Li Y. Circulating exosomal microRNAs as prognostic biomarkers for non-small-cell lung cancer. Oncotarget 2017; 8: 13048-13058.

[9] Pua HH, Happ HC, Gray CJ, Mar DJ, Chiou NT, Hesse LE and Ansel KM. Increased hematopoietic extracellular RNAs and vesicles in the lung during allergic airway responses. Cell Rep 2019; 26: 933-944.

[10] Xu H, Ling M, Xue J, Dai X, Sun Q, Chen C, Liu Y, Zhou L, Liu J, Luo F, Bian Q and Liu Q. Exosomal microRNA-21 derived from bronchial epithelial cells is involved in aberrant epithelium-fibroblast cross-talk in COPD induced by cigarette smoking. Theranostics 2018; 8: 5419-5433.

[11] Du Y, Ding Y, Chen X, Mei Z, Ding H, Wu Y and Jie Z. MicroRNA-181c inhibits cigarette smoke-induced chronic obstructive pulmonary disease by regulating CCN1 expression. Respir Res 2017; 18: 155.

[12] Sundar IK, Li D and Rahman I. Small RNA-sequence analysis of plasma-derived extracellular vesicle miRNAs in smokers and patients with chronic obstructive pulmonary disease as

circulating biomarkers. J Extracell Vesicles 2019; 8: 1684816.
[13] Su J, Li J, Lu Y, Li N, Li P, Wang Z, Wu W and Liu X. The rat model of COPD skeletal muscle dysfunction induced by progressive cigarette smoke exposure: a pilot study. BMC Pulm Med 2020; 20: 74.
[14] Li P, Kaslan M, Lee SH, Yao J and Gao Z. Progress in exosome isolation techniques. Theranostics 2017; 7: 789-804.
[15] Wu X, Showiheen S, Sun AR, Crawford R, Xiao Y, Mao X and Prasadam I. Exosomes extraction and identification. Methods Mol Biol 2019; 2054: 81-91.
[16] Liang GB and He ZH. Animal models of emphysema. Chin Med J (Engl) 2019; 132: 2465-2475.
[17] Sokar SS, Afify EH and Osman EY. Dexamethasone and losartan combination treatment protected cigarette smoke-induced COPD in rats. Hum Exp Toxicol 2021; 40: 284-296.
[18] Pegtel DM and Gould SJ. Exosomes. Annu Rev Biochem 2019; 88: 487-514.
[19] Vlassov AV, Magdaleno S, Setterquist R and Conrad R. Exosomes: current knowledge of their composition, biological functions, and diagnostic and therapeutic potentials. Biochim Biophys Acta 2012; 1820: 940-948.
[20] Kaur G, Maremanda KP, Campos M, Chand HS, Li F, Hirani N, Haseeb MA, Li D and Rahman I. Distinct exosomal miRNA profiles from BALF and lung tissue of COPD and IPF patients. Int J Mol Sci 2021; 22: 11830.
[21] Singh KP, Maremanda KP, Li D and Rahman I. Exosomal microRNAs are novel circulating biomarkers in cigarette, waterpipe smokers, E-cigarette users and dual smokers. BMC Med Genomics 2020; 13: 128.
[22] Fujita Y, Araya J, Ito S, Kobayashi K, Kosaka N, Yoshioka Y, Kadota T, Hara H, Kuwano K and Ochiya T. Suppression of autophagy by extracellular vesicles promotes myofibroblast differentiation in COPD pathogenesis. J Extracell Vesicles 2015; 4: 28388.
[23] Wen H, Liu Z, Tang J and Bu L. MiR-185-5p targets RAB35 gene to regulate tumor cell-derived exosomes-mediated proliferation, migration and invasion of non-small cell lung cancer cells. Aging (Albany NY) 2021; 13: 21435-21450.
[24] Değerli E, Torun V and Cansaran-Duman D. MiR-185-5p response to usnic acid suppresses proliferation and regulating apoptosis in breast cancer cell by targeting Bcl2. Biol Res 2020; 53: 19.
[25] Xu L, Yi M, Tan Y, Yi Z and Zhang Y. A comprehensive analysis of microRNAs as diagnostic biomarkers for asthma. Ther Adv Respir Dis 2020; 14: 1753466620981863.
[26] Rodrigo-Muñoz JM, Cañas JA, Sastre B, Gil-Martínez M, García LR, Sastre J and Del PV. Role of miR-185-5p as modulator of periostin synthesis and smooth muscle contraction in asthma. J Cell Physiol 2022; 237: 1498-1508.
[27] He W, Su X, Chen L, Liu C, Lu W, Wang T and Wang J. Potential biomarkers and therapeutic targets of idiopathic pulmonary arterial hypertension. Physiol Rep 2022; 10: e15101.
[28] Zhong XQ, Yan Q, Chen ZG, Jia CH, Li XH, Liang ZY, Gu J, Wei HL, Lian CY, Zheng J and Cui QL. Umbilical cord blood-derived exosomes from very preterm infants with bronchopulmonary dysplasia impaired endothelial angiogenesis: roles of exosomal microRNAs. Front Cell Dev Biol 2021; 9: 637248.
[29] Wu X, Wang W, Wu G, Peng C and Liu J. MiR-182-5p serves as an oncogene in lung adenocarcinoma through binding to STARD13. Comput Math Methods Med 2021; 2021: 7074343.
[30] Cao MQ, You AB, Zhu XD, Zhang W, Zhang YY, Zhang SZ, Zhang KW, Cai H, Shi WK, Li XL, Li KS, Gao DM, Ma DN, Ye BG, Wang CH, Qin CD, Sun HC, Zhang T and Tang ZY. MiR-182-5p promotes hepatocellular carcinoma progression by repressing FOXO3a. J Hematol Oncol 2018; 11: 12.
[31] Chen Y, Zhang Q, Zhou Y, Yang Z and Tan M. Inhibition of miR-182-5p attenuates pulmonary fibrosis via TGF-β/Smad pathway. Hum Exp Toxicol 2020; 39: 683-695.
[32] Dang X, He B, Ning Q, Liu Y, Chang Y and Chen M. Suppression of TRIM8 by microRNA-182-5p restricts tumor necrosis factor-α-induced proliferation and migration of airway smooth muscle cells through inactivation of NF-κB. Int Immunopharmacol 2020; 83: 106475.
[33] Xiao K, He W, Guan W, Hou F, Yan P, Xu J, Zhou T, Liu Y and Xie L. Mesenchymal stem cells reverse EMT process through blocking the activation of NF-κB and Hedgehog pathways in LPS-induced acute lung injury. Cell Death Dis 2020; 11: 863.